

# Discrete modulational instability in periodically poled lithium niobate waveguide arrays

Robert Iwanow and George I. Stegeman

College of Optics and Photonics, CREOL/FPCE, University of Central Florida  
4000 Central Florida Blvd., Orlando, FL 32816-2700, USA  
[george@creol.ucf.edu](mailto:george@creol.ucf.edu)

Roland Schiek

University of Applied Sciences Regensburg, Prüfening Str. 58, 93049 Regensburg, Germany

Yoohong Min and Wolfgang Sohler

University of Paderborn, D-33095 Paderborn, Germany

**Abstract:** Parametric gain associated with discrete modulational instability due to the second order nonlinearity  $\chi^{(2)}(-2\omega; \omega, \omega)$  was investigated experimentally in periodically poled lithium niobate arrays of weakly coupled channel waveguides for conditions of both positive and negative phase-mismatch for second harmonic generation.

© 2005 Optical Society of America

**OCIS codes:** (190.2620) Frequency conversion; (190.4390) Nonlinear optics, integrated optics; (190.5530) Pulse propagation and solitons; (190.5940) Self-action effects

---

## References and Links

1. N. N. Akhmediev and A. Ankiewicz, *Solitons: Nonlinear Pulses and Beams* (Chapman and Hall, London, 1997).
2. E. Infeld and G. Rowlands, *Nonlinear Waves, Solitons and Chaos* (Cambridge University Press, Cambridge, 1990).
3. R. A. Fuerst, D. M. Baboiu, B. Lawrence, W. E. Torruellas, G. I. Stegeman, and S. Trillo, "Spatial modulational instability and multisoliton-like generation in a quadratically nonlinear optical medium," *Phys. Rev. Lett.* **78**, 2756-2759 (1997).
4. R. Malendevich, L. Jankovic, G. I. Stegeman, and J. S. Aitchison, "Spatial modulation instability in a Kerr slab waveguide," *Opt. Lett.* **26**, 1879-1881 (2001).
5. D. Kip, M. Soljacic, M. Segev, E. Eugenieva, and D. N. Christodoulides, "Modulation instability and pattern formation in spatially incoherent light beams," *Science* **290**, 495-498, (2000).
6. H. S. Eisenberg, Y. Silberberg, R. Morandotti, A. R. Boyd, and J. S. Aitchison "Discrete spatial optical solitons in waveguide arrays," *Phys. Rev. Lett.* **81**, 3383-3386 (1998).
7. J. W. Fleischer, M. Segev, N. K. Efremidis, and D. N. Christodoulides, "Observation of two-dimensional discrete solitons in optically-induced nonlinear photonic lattices," *Nature* **422**, 147-150 (2003).
8. R. Iwanow, R. Schiek, G. Stegeman, T. Pertsch, F. Lederer, Y. Min, and W. Sohler, "Observation of discrete quadratic solitons," *Phys. Rev. Lett.* **93** 113902 (2004).
9. D. N. Christodoulides, F. Lederer, and Y. Silberberg, "Discretizing light behaviour in linear and nonlinear waveguide lattices," *Nature* **424**, 817-823 (2003).
10. D. N. Christodoulides and R. I. Joseph, "Discrete self-focusing in nonlinear arrays of coupled waveguides," *Opt. Lett.* **13**, 794-796 (1988); Y. S. Kivshar and M. Peyrard, "Modulational instabilities in discrete lattices," *Phys. Rev. A* **46**, 3198-3205 (1992).
11. J. Meier, G. I. Stegeman, D. N. Christodoulides, Y. Silberberg, R. Morandotti, G. Salamo, and J.S. Aitchison, "Experimental Observation of Discrete Modulational Instability," *Phys. Rev. Lett.* **92**, 163902, (2004).
12. A. V. Buryak, P. Di Trapani, D. Skryabin, and S. Trillo, "Optical solitons due to quadratic nonlinearities: from basic physics to futuristic applications," *Phys. Reports* **370**, 63-235 (2002).
13. G.I. Stegeman, D.J. Hagan, and L. Torner, " $\chi^{(2)}$  Cascading phenomena and their applications to all-optical signal processing, mode-locking, pulse compression and solitons," *J. Opt. Quantum Electron.* **28**, 1691-1740 (1996).

## 1. Introduction

The most fundamental consequence of propagating high intensity, plane waves beams in bulk optically nonlinear media is that filamentation due to any amplitude or phase noise present on the beam occurs for media with an effective self-focusing nonlinearity but not in media with negative (defocusing) nonlinearities [1,2]. Such phenomena have been observed in a variety of continuous nonlinear optical media, the behavior having many universal properties because diffraction has only one sign in continuous media [3-5].

The nonlinear behavior of beams in discrete media consisting of arrays of weakly coupled channel waveguides has been of recent interest in cubic, quadratic and photorefractive media [6-8]. A large variety of discrete solitons has been predicted, and many have been observed experimentally [9]. One of the reasons for this proliferation of spatial solitons when compared to that found in continuous media is that the one-dimensional dispersion relation linking the longitudinal ( $k_x$ ) and transverse ( $k_y$ , Bloch) wavevectors where  $x$  is the channel direction, is sinusoidal in nature so that the diffraction coefficient  $D = d^2k_x/dk_y^2$  can be either normal (negative as in continuous media) or anomalous (positive with no analog in continuous media). For a self-focusing nonlinearity, filamentation is expected to occur for regions of normal diffraction and to be absent for regions of anomalous diffraction [10]. This diversity of behavior forbidden in continuous media has been reported recently in 1D arrays of AlGaAs channel waveguides which exhibit self-focusing Kerr nonlinearities [11]. However, there have been no experiments on filamentation reported for self-defocusing nonlinearities in discrete media, nor in quadratically nonlinear media whose nonlinearity can be either focusing or defocusing.

Quadratically nonlinear media play a unique role in soliton science because their solitons consist of all the frequency components, two or three, which are strongly coupled in a parametric interaction based on quadratic nonlinearities [12]. Discrete quadratic solitons associated with second harmonic generation (SHG) have been observed in arrays of periodically poled lithium niobate waveguides [8]. In those arrays, not only can the sign of diffraction for the fundamental beam be changed by varying the propagation direction ( $k_y$ ) across the array, but also the sign of the effective focusing or defocusing nonlinearity by varying the phase-mismatch condition for the parametric interaction [13]. Therefore, although filamentation also occurs for normal incidence in quadratic media with a self-focusing nonlinearity (positive wavevector mismatch), in contrast to the AlGaAs case, filamentation should be eliminated by simply tuning the wavevector-mismatch to negative values. Here we demonstrate for normal incidence onto quadratically nonlinear waveguide arrays the existence of parametric gain associated with modulational instability for self-focusing nonlinearities, and its absence in the defocusing case.

## 2. Experimental details

The sample consisted of waveguide arrays containing 101 guides fabricated on 70mm long Z-cut LiNbO<sub>3</sub> wafers by diffusing 7 $\mu$ m wide Ti stripes of 90nm thickness into the substrate for 8.5 hours at 1060°C [8]. Waveguides with losses of 0.2dB/cm for the FW and 0.4dB/cm for the SH were obtained. For efficient SHG phase-matching between the FW (1550nm) TM<sub>00</sub> and the SH (775nm) TM<sub>00</sub> waveguide modes at ~200°C, a uniform QPM grating (ferroelectric domain structure) of 16.75 $\mu$ m periodicity was written in the sample by electric field poling. The center-to-center spacing  $d$  between the array's channels was 15 $\mu$ m. The phase-matching condition was tuned by varying the wavelength of an OPG/OPA from 1547 to 1565nm. The bandwidth of the OPG/OPA was 0.4nm, larger than the SHG bandwidth of 0.25nm measured in individual "witness" channels surrounding the associated the array. The arrays were housed in an oven and heated to temperatures of 200°C in order to avoid photorefractive damage. The combination of sample length and number of channels in an array limited the angular range of propagation that could be followed at the output end of the 7cm long sample without reflections occurring at the array boundaries.

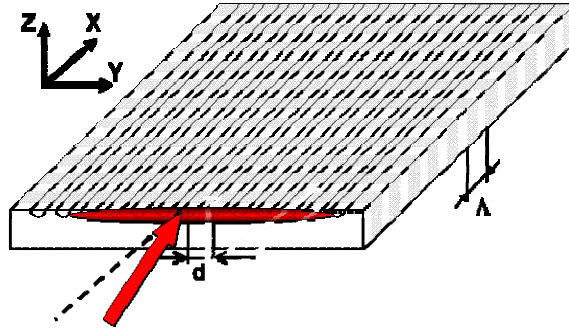


Fig. 1. Geometry of the wide, high intensity fundamental beam interacting with a PPLN array near its phase-matching condition for second harmonic generation.

The light-sample geometry of interest is shown in Fig. 1. The broad input fundamental beam whose wavelength was varied from 1547 to 1565 nm was obtained from an EKSPLA OPG/OPA pumped by an EKSPLA Nd:YAG laser producing 15ps pulses with energies up to 200μJ with energy stability of ±15%. A lens train was used to produce a highly elliptical beam approximately Gaussian in shape in two dimensions with a planar wavefront at the sample's input facet. The beam dimensions were 350μm x 3.5μm along the 1D array and in the dimension orthogonal to the surface respectively. The beam's full width at half-maximum covered 23 channels at the input. In this setting, 1μJ pulse corresponds to a peak power of 2.3kW and peak intensity of 13GW/cm<sup>2</sup> in the middle channel. Provision was also provided for tilting the input beam by small angles (a few degrees) around an axis orthogonal to the surface normal in order to vary the relative input phase  $k_y d$  between adjacent channels.

The two key parameters which govern discrete diffraction are the propagation distance required for complete transfer between two coupled, but otherwise isolated channels, i.e. the coupling length  $L_C$ , and the general form of the dispersion ( $k_x$  versus  $k_y$ ). They were measured for the fundamental beam at room temperature. By monitoring the centroid of the output fundamental beam as a function of the relative phase angle  $k_y d$  at which the input beam is launched, the angular dependence of  $dk_x/dk_y$  was measured. The results are shown in Fig. 2. Clearly the diffraction coefficient ( $\propto d^2 k_x/dk_y^2$ ) has zeros in this sample at  $k_y d = \pm\pi/2$ , as given by simple nearest-neighbors couple mode theory. By measuring the discrete diffraction for single channel inputs and matching to theory, a linear coupling length of 15.74mm was deduced for the FW. As discussed previously, the tight spatial confinement of the second harmonic fields leads to SH coupling lengths much longer than the sample length so that  $k_x$  is independent of  $k_y$  for the harmonic component [8]. This also means that there is no discrete diffraction of the SH and it remains in the channel in which it is generated.

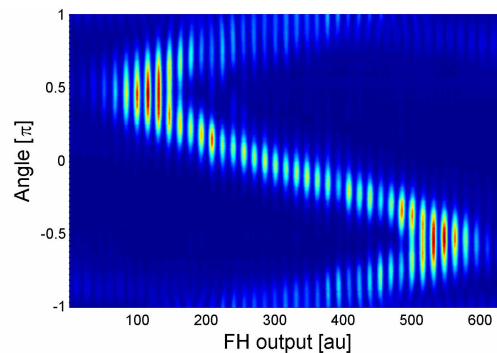


Fig. 2. The first derivative  $dk_y/dk_x$  of the dispersion relation obtained by plotting the centroid at the output facet of a fundamental beam injected into the PPLN arrays as a function of the relative phase between the adjacent channels.

### 3. Modulation instability at normal incidence

The first nonlinear experiments consisted of directing the input fundamental beam at normal incidence ( $k_y d = 0$  - normal diffraction) onto the array for both positive and negative wavevector mismatch. The beam observed emerging from the output facet was measured as a function of increasing fundamental input energy and is shown in Fig. 3. Total output energy was normalized to the same value for different input energies.

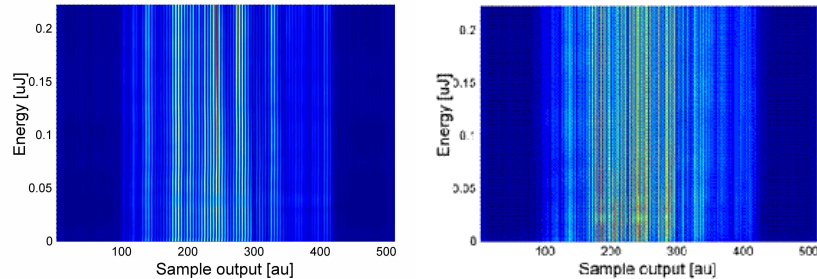


Fig. 3 Output from PPLN array as a function of increasing input fundamental energy. Left-hand-side: positive phase-mismatch of  $170\pi$ . Right-hand-side: negative phase-mismatch of  $-40\pi$ .

Here waveguide imperfections play the role of an amplitude “seed”. In the defocusing case it is clear that the output pattern is independent of increasing power, i.e. no filamentation growth occurs due MI parametric gain and instead the pattern contrast decays due to propagation losses. For positive wavevector mismatch (self-focusing case), the relative intensity of the defect seeded channels increases. Plotted in Fig. 4 is the spatial Fourier spectrum of the normalized output shown in Fig. 3.

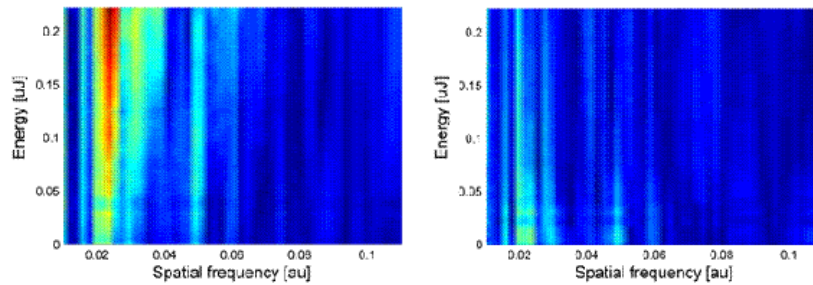


Fig. 4. Spatial Fourier transform of the output intensity patterns shown in Fig. 3.. Left-hand-side: positive phase-mismatch of  $170\pi$ . Right-hand-side: negative phase-mismatch= $-40\pi$ .

There is clearly gain in the self focusing case for a Fourier component representing the defects followed by saturation due to the long samples used. In contrast, for the defocusing case there is no increase in Fourier components with increasing power. The corresponding normalized output intensity distributions are shown in Fig. 5 at low (blue) and high (green) powers. Clearly a periodic pattern occurs at high powers for the self-focusing case where-as no pattern emerges for the defocusing case. Note that moving from one limit to the other just involved a change in the input wavelength.

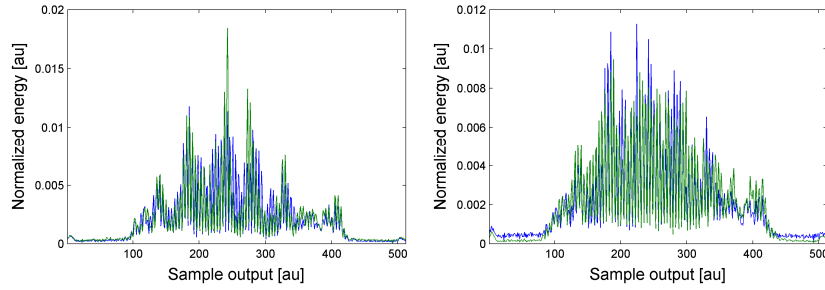


Fig. 5. Low and high power output intensity distribution from the array at high (green) and low (blue) powers. Left-hand-side: positive phase-mismatch of  $170\pi$ . Right-hand-side: negative phase-mismatch of  $-40\pi$ .

Simulations were also performed to verify theoretically that MI only occurs for the self-focusing case at normal incidence. The system is described by the equations:

$$i \frac{\partial u_n}{\partial z} + i \delta \frac{\partial u_n}{\partial t} + c(u_{n+1} + u_{n-1}) + 2\gamma u_n^* v_n = 0$$

$$i \frac{\partial v_n}{\partial z} - \Delta\beta v_n + \gamma u_n^2 = 0,$$

where  $u_n$  and  $v_n$  are the fundamental and harmonic fields at the center of the  $n$ 'th channel, and  $c$ ,  $\delta$ ,  $\Delta\beta$  and  $\gamma$  represent the linear coupling constant, the inverse group velocity mismatch, linear wavevector mismatch and the effective quadratic nonlinear coefficient, respectively. Note that the SH field inter-channel coupling can be neglected for the simulation of our experiment as the coupling of the SH is much weaker than for the FW because of the much tighter SH mode confinement in the channels. The results in Fig. 6 obtained for the experimental parameters verify that parametric amplification should occur for the self-focusing case, but not for the self-defocusing case, as observed experimentally.

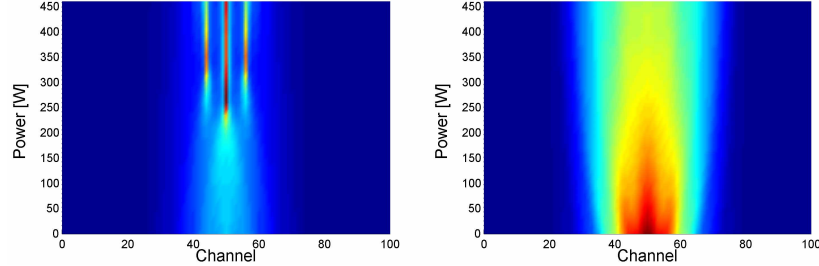


Fig. 6. Calculated evolution of a seeded fundamental beam in the PPLN array as a function of increasing peak input fundamental power in the middle channel. Experimental parameters were assumed. Left-hand-side: positive phase-mismatch of  $170\pi$ . Right-hand-side: negative phase-mismatch of  $-40\pi$ .

#### 4. Measurements at non-normal incidence

The effect of varying the relative input phase  $k_y d$  through the zero diffraction point was also investigated. These measurements were limited by a number of factors. Reflections that occur at the array boundaries due to the large sample lengths and the total number of channels in an array limit the angular range to  $|k_y d| \leq 0.75\pi$ . The lack of second harmonic coupling between adjacent channels and therefore the resulting difference in the fundamental and harmonic dispersion relations limits the growth of the harmonic. Furthermore, small variations in SH generation efficiencies between channels found experimentally lead to cumulative phase variations in the fundamental along the channel. Nevertheless, it is clear from the high input power pictures in Fig. 7 that, for positive wavevector mismatch, filamentation only occurs for  $|k_y d| \leq 0.5\pi$  (i.e. normal diffraction) and disappears for  $|k_y d| \geq 0.5\pi$  (anomalous diffraction).

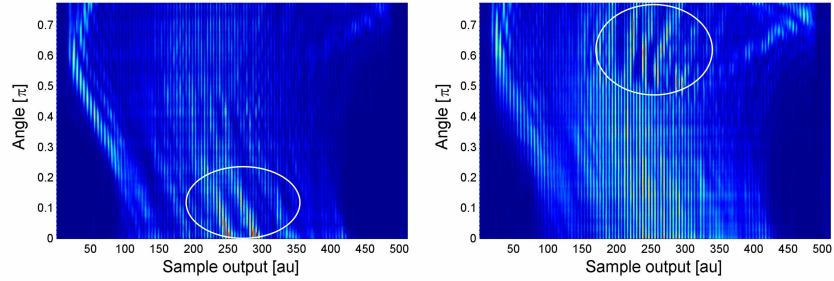


Fig. 7. Distribution across the array of the fundamental beam output power from the PPLN array for incidence of the fundamental beam as a function of the relative input phase between adjacent channels. Positive phase mismatch =  $170\pi$  on the left; negative phase-mismatch =  $-40\pi$  on the right. The input pulse energy was  $0.27\mu\text{J}$  corresponding to a peak power of  $620\text{W}$  in the middle channel. Regions of high contrast filaments are identified by ellipses.

In contrast to this, for negative wavevector mismatch, no filamentation occurs for  $|k_y d| \leq 0.5\pi$  but does occur for  $|k_y d| \geq 0.5\pi$ . All of these results are consistent with filamentation when the product of the diffraction coefficient ( $D$ ) and the wavevector mismatch is negative, and no filamentation when the product is positive. The results are also in agreement with the previous experiments on filamentation observed due to the self-focusing Kerr nonlinearity in AlGaAs arrays [11].

## 5. Summary

In summary, we have observed MI gain due to discrete modulation instability in arrays with quadratic nonlinearities. Whether filamentation occurs or not depends on the sign of the product of the diffraction coefficient and the cascading nonlinearity

This research was supported in the U.S. by the National Science Foundation and an ARO MURI on Solitonic Gateless Computing, and in Europe by the European Community project ROSA (IST-2000-26005).